

Measurements of ultracold neutron upscattering and absorption in polyethylene and vanadium.

E. I. Sharapov,¹ C. L. Morris,^{2,*} M. Makela,² A. Saunders,² Evan R. Adamek,³ Y. Bagdasarova,² L. J. Broussard,² C. B. Cude-Woods,³ Deon E Fellers,² Peter Geltenbort,⁴ S. I. Hasan,⁵ K. P. Hickerson,⁶ G. Hogan,² A. T. Holley,³ Chen-Yu Liu,³ M. P. Mendenhall,⁶ J. Ortiz,² R. W. Pattie Jr.,⁷ D. G. Phillips II,⁷ J. Ramsey,² D. J. Salvat,³ S. J. Seestrom,² E. Shaw,² Sky Sjue,² W. E. Sondheim,² B. VornDick,⁷ Z. Wang,² T. L. Womack,² A. R. Young,⁷ and B. A. Zeck⁷

¹*Joint Institute for Nuclear Research, 141980, Dubna, Russia*

²*Los Alamos National Laboratory, Los Alamos, NM 87544, USA*

³*Department of Physics, Indiana University, Indiana 47405-7105 USA*

⁴*Institut Laue-Langevin, 38042 Grenoble Cedex 9, France*

⁵*Department of Physics and Astronomy, University of Kentucky, Lexington, Kentucky 40506, USA*

⁶*Kellogg Radiation Laboratory, California Institute of Technology, Pasadena, California 91125, USA.*

⁷*Department of Physics, North Carolina State University, Raleigh, North Carolina 27695, USA*

(Dated: May 31, 2013)

The study of neutron cross sections for elements used as efficient “absorbers” of ultracold neutrons (UCN) is crucial for many precision experiments in nuclear and particle physics, cosmology and gravity. In this context, “absorption” includes both the capture and upscattering of neutrons to the energies above the UCN energy region. The available data, especially for hydrogen, do not agree between themselves or with the theory. In this report we describe measurements performed at the Los Alamos National Laboratory UCN facility of the UCN upscattering cross sections for vanadium and for hydrogen in CH₂ using simultaneous measurements of the radiative capture cross sections for these elements. We measured $\sigma_{up} = 1972 \pm 130$ b for hydrogen in CH₂, which is below theoretical expectations, and $\sigma_{up} < 25 \pm 9$ b for vanadium, in agreement with the expectation for the neutron heating by thermal excitations in solids.

PACS numbers: 25.40.Fq, 25.40.Kv, 28.20.Ka

Several recent reviews highlight the application of ultracold neutrons in past and ongoing experiments for searching for the neutron electric dipole moment [1], for precision measurement of the neutron lifetime [2], for neutron β -decay correlations [3] and for gravitational quantum states [4], as well as for solving new issues in cosmology [5]. Ultracold neutrons greatly increase the sensitivity of experiments because they can be confined in the apparatus for times comparable with the neutron lifetime owing to the action of the ‘optical’ Fermi potential, U_F ,

$$U_F = \frac{2\pi\hbar^2}{m}Nb, \quad (1)$$

where m is the neutron mass, N is the number density of the material, and b is the neutron scattering length.

Materials with high positive potential, $U_F \simeq 250$ neV, are used for trapping UCN because neutrons with kinetic energy lower than that value are reflected from walls at all angles of incidence. The velocity of such neutrons is below 7 m/s. On the other hand, materials made from elements with a small negative optical potential, like hydrogen, vanadium, titanium serve for removal of UCN through absorption and/or upscattering to higher energy. The efficiency of this removal is important for many measurements and this continues to motivate the study of such materials. Vanadium and hydrogen are perfect neutron incoherent scatterers, and both have small negative, practically non-reflective potential $U_F \simeq -7.1$ neV. For these elements, the theory of upscattering in one-phonon incoherent approximation is usually applied in the theory of upscattering, and the UCN isotropic differential upscattering cross section for cubic lattices can be calculated by a simple formula [6]:

$$\frac{d\sigma_{up}}{dE} = \sigma_b \sqrt{\frac{E}{E_i}} \left(e^{E/kT} - 1 \right)^{-1} \frac{g(E)}{A} e^{-2W}, \quad (2)$$

where $\sigma_b = 4\pi b^2$ is the cross section for bound nuclei with the mass number A , E_i is the initial UCN energy, E is the energy after upscattering, $g(E)$ is the phonon density of states and the last exponent is the Debye-Waller factor

*Corresponding author; Electronic address: morris@lanl.gov

which is often measured, although it can be calculated as well. The MCNP code [7] with the thermal data kernels for the scattering law $S(\alpha, \beta)$ (α and β are the reduced momentum and energy transfers) calculates the neutron inelastic scattering cross section corrected for multi-phonon contributions to Eq.(2) when applicable. The cross sections for several neutron moderators have been calculated using MCNP by [8]. For polyethylene, at the minimum evaluated energy of 0.01 meV ($v=43.7$ m/s) the upscattering cross section is $\sigma_{up} = 320$ b and the $1/v$ law applies below $\simeq 0.1$ meV.

Total neutron cross sections for vanadium have been measured over the velocity range from 4.4 m/s to 17.7 m/s in [9]. The inferred capture cross section was analyzed together with other thermal data and was shown to follow the expected $1/v$ law up to thermal velocities, 2200 m/s. With this result and with the thermal value $\sigma_a = 4.92 \pm 0.05$ barn [10] for the isotope ^{51}V , we write $\sigma_a\sqrt{E} = 0.808 \pm 0.008$ b $eV^{1/2}$. The vanadium upscattering cross section σ_{up} has not been measured but has been estimated [11] in the one-phonon approximation to follow the $1/v$ law below $\simeq 0.1$ meV with the value $\sigma_{up}\sqrt{E} = 0.012 \pm 0.002$ b $eV^{1/2}$, giving the relative contribution of the upscattering cross section at the level of 1.5%. The capture cross section for ^{51}V is large at UCN energies, 2700 b for UCN at 4 m/s velocity. For hydrogen the relationship between absorption and upscattering is reversed: the average UCN upscattering cross section, according to the measurement [12], is 3745 ± 370 b while the thermal cross section value $\sigma_a = 0.3326 \pm 0.0007$ [10] and the $1/v$ law leads to $\sigma_a(4\text{m/s}) = 182.9$ b. Lower upscattering cross sections values for hydrogen in polyethylene have been obtained from the recent UCN time-of-flight measurements [13], where the $\sigma_{up}(E)$ was shown to follow the $1/v$ law with the value $\sigma_{up}(4\text{m/s}) = 2053 \pm 40$ b, at 4 m/s. The reasons for the disagreement between the results of measurements [12] and [13] remain unclear.

Measurements of the UCN upscattering and capture cross sections have been performed using the Los Alamos National Laboratory solid-deuterium ultracold neutron source driven by an 800-MeV, 5 μA average proton beam provided by the Los Alamos Neutron Science Center(LANSCE) linear accelerator. The source is described in detail in a recent publication by Saunders et al. [14]. The UCN density in the stainless steel guide after the source exit window was $\simeq 1$ UCN/cm³. The UCN velocity spectrum was cut off by the $U_F = 189$ neV potential. Our Monte Carlo modeling of the UCN transport in the source and guides [14] suggests a velocity spectrum $n(v) \sim v^3 dv$ below cutoff, rather than a Maxwellian distribution $v^2 dv$ because of absorption in the thick solid deuterium source. This number was lower than typical because these measurements were made with non-ideal source conditions, low volume and high para-deuterium contamination. The cross sections obtained in this experiment, which are averaged over the UCN velocity spectrum, corresponds to the average velocity $v_{av} \simeq 4$ m/s (the UCN energy $\simeq 80$ neV). Upscattering and capture have been measured simultaneously. The beam intensity during vanadium and hydrogen runs was monitored by our standard UCN monitor [14]. The gamma rays from neutron radiative capture in hydrogen and vanadium were measured in a 100% efficient (relative to a 7.6 cm \varnothing by 7.6 cm thick right circular cylinder of NaI) high purity germanium detector (HPGe). The neutron detector for the upscattering measurement was a 30 cm long drift tubes [15] with 1.8 bar of ^3He and 1 bar of CF_4 . Both detectors were placed outside of the 7.5 cm diameter UCN guide upstream of the target location. The thicknesses of the targets, 0.25 mm of vanadium, and 1.6 mm of polyethylene, were chosen to absorb all neutrons that enter the materials. The target foils were backed by a nickel foil ($U_F(\text{Ni}) \simeq 250$ neV) between them and the end of a UCN guide, reflecting any transmitted UCN neutrons back into the sample. The weak reflections from the vanadium and polyethylene surfaces are nearly equal and negligible for UCN with perpendicular energies higher than $\simeq 5$ neV.

In Fig. 1 pulse height spectra from the neutron detector for the two targets are compared to a run with no target. The upscatter rate with the polyethylene target is much larger than with the vanadium target. Both targets produce upscatter neutron rates significantly above the background, which was mostly due to cosmogenic thermal background. The background associated with the proton beam was eliminated using time gates on the analog to digital converters, to reject events during the beam pulses. The relative neutron rates were calculated by integrating the spectra shown in Fig. 2 and subtracting the background measured with an empty target. The efficiencies of the ^3H detector for neutron spectra up scattered by CH_2 and V have been modeled using spectral data of [16] and found to be equal with the accuracy of 2%.

In the measurement with the HPGE detector a large number of γ -ray lines were observed with both the vanadium and the polyethylene foils. With the polyethylene foil many of the lines were due to up scattered neutrons capturing in the materials of the detector. With the vanadium foil there are a large number of capture lines extending up to 8 MeV. Two γ -ray lines have been used in the current analysis, the 2.225 MeV n-p capture line and the 1.434 MeV γ ray emitted in the decay of ^{52}V . The HPGe photopeak efficiencies for them in our geometry have been modeled by the MCNP5 code with the result $\epsilon(1.434) = 1.37 \epsilon(2.225)$. The γ rate from the decay of the isotope ^{52}V produced by neutron capture builds up to equilibrium with a time constant given by the lifetime of ^{52}V of 5.4 minutes. Equilibrium was ensured by waiting for two lifetimes with the beam on target before starting measurements with the vanadium target. The resulting spectra are shown in Fig. 2. Rates were extracted by

subtracting the background measured using the alternate target. The empty runs were not useful for these because of the large increase in background due to Compton events from other capture induced processes in the detector.

TABLE I: Neutron r_n and gamma ray r_a count per 300 s, their ratios $R(V/H)$ and the obtained UCN scattering cross sections σ_n for the Vanadium target and Hydrogen in the polyethylene target. The gamma ray ratio has been corrected for the relative efficiency for the vanadium(1.44 MeV) and hydrogen capture (2.22 MeV) lines. The absorption cross sections σ_a , used in the analysis, are obtained by applying the $1/v$ law to thermal data from [10].

Targets and $R(V/H)$	r_n	r_a	$\sigma_n(4 \text{ m/s}), \text{ b}$	$\sigma_a(4 \text{ m/s}), \text{ b}$
Vanadium (V)	19 ± 5	10590 ± 11	25 ± 9	2706 ± 0.27
Polyethylene (H)	1869 ± 22	871 ± 40	2062 ± 135	182.9 ± 0.4
$R_n(V/H)$	0.010 ± 0.003			
$R_a(V/H)$		12.16 ± 0.7		

The data were analyzed as follows. Because all the incident UCN on V and CH_2 are either captured or scattered, the relative contributions of these processes are given by the ratios σ_a/σ_t and σ_n/σ_t , where the total cross section σ_t is the sum $\sigma_t = \sigma_n + \sigma_a$. The counting rates of the capture and neutron detectors, r_a and r_n , corrected for efficiencies in the V and H targets are

$$r_a = \frac{\sigma_a}{\sigma_t} \Phi S \epsilon_a, \quad r_n = \frac{\sigma_n}{\sigma_t} \Phi S \epsilon_n, \quad (3)$$

where Φ is the neutron fluence (the same for both targets after normalizing on the UCN monitor), S is the target area (the same for both targets), ϵ_a and ϵ_n are the corresponding detectors efficiencies (including the solid angles) and we omitted, for simplicity, the indices of targets.

Introducing the ratios between vanadium and hydrogen count rates

$$R_a \equiv \frac{r_a(V)}{r_a(H)} = \frac{\sigma_a(V)}{\sigma_t(V)} \frac{\sigma_t(H)}{\sigma_a(H)}, \quad (4)$$

and

$$R_n \equiv \frac{r_n(V)}{r_n(H)} = \frac{\sigma_n(V)}{\sigma_t(V)} \frac{\sigma_t(H)}{\sigma_n(H)}, \quad (5)$$

we obtain the relationship between the measured V and H cross sections.

$$\frac{\sigma_a(V)}{\sigma_n(V)} = \frac{R_a}{R_n} \frac{\sigma_a(H)}{\sigma_n(H)}. \quad (6)$$

To obtain relationships between σ_a and σ_n for each target separately one has to estimate the quantities $(1 - R_n)$ and $(R_a - 1)$ making use of the inequality $\sigma_a(V) \gg \sigma_n(V)$. The result for hydrogen is

$$\frac{\sigma_a(H)}{\sigma_n(H)} = \frac{(1 - R_n)}{(R_a - 1)}, \quad (7)$$

and, after substitution it into Eq. (6), the result for vanadium is

$$\frac{\sigma_a(V)}{\sigma_n(V)} = \frac{R_a (1 - R_n)}{R_n (R_a - 1)}. \quad (8)$$

The experimental results obtained from this analysis are given in Table I. From these data the UCN upscattering cross section on hydrogen, taken as the difference between the measured total scattering cross section σ_n and the known (90 b) elastic σ_{el} cross section, is $\sigma_{up}(4 \text{ m/s}) = 1972 \pm 130 \text{ b}$. Our measurements support recent TOF measurements of Pokotilovski et al. [13], but disagree with the measurements of Zhukov et al. [12], which served the UCN community for a long time as the only experimental data on upscattering in CH_2 . It should be noted that our MCNP calculations [8] of σ_{up} for CH_2 agree with [12] in disagreement with our experimental result. Our result for vanadium is the first experimental confirmation of the extremely low UCN upscattering in V and, in this case, agrees

with the theory of UCN heating by phonons in solids.

Acknowledgment This work was performed under the auspices of the U.S. Department of Energy under Contract DE-AC52-06NA25396. Author DJS is supported by the DOE Office of Science Graduate Fellowship Program (DOE SCGF), made possible in part by the American Recovery and Reinvestment Act of 2009, administered by ORISE-ORAU under contract no. DE-AC05-06OR23100.

-
- [1] S. K. Lamoreaux and R. Golub, J. Phys. G: Nucl. Part. Phys. **36**, 104002 (2009).
 - [2] Fred E. Wietfeldt and Geoffrey L. Greene, Rev. Mod. Phys. **83**, 1173 (2011).
 - [3] Hartmut Abele, Progress in Particle and Nuclear Physics **60**, 1 (2008).
 - [4] Valerii V. Nesvizhevsky, Physics-Uspekhi **53**, 645 (2010).
 - [5] D. Dubbers and M. G. Schmidt, Rev. Mod. Phys. **83**, 1111 (2011).
 - [6] I. I. Gurevich, L. V. Tarasov, *Low-energy neutron physics* (North-Holland Publishing Company, Amsterdam, 1968).
 - [7] X-5-Monte-Carlo-team, MCNP – a General Monte Carlo N-Particle Transport Code, Version 5, Report No. LA-UR-03-198, Los Alamos National Laboratory, Los Alamos 2003.
 - [8] D. E. Cullen, L. F. Hansen, E. M. Lent, E. F. Plecharty, Report UCRL-ID-153656, Lawrence Livermore National Laboratory, Livermore 2003. Available from <http://www.llnl.gov/tid/Library.html>
 - [9] J. A. Polo and J. M. Robson, Phys. Rev. C **27**, 133 (1983).
 - [10] S. F. Mughabghab, *Atlas of Neutron Resonances: Resonance Parameters and thermal cross sections Z=1–100* (Elsevier, Amsterdam, 2006).
 - [11] W. Dilg and W. Mannhart, Z. Physik **266**, 157 (1974).
 - [12] S. W. Zhukov, V. L. Kuznetsov, V. I. Morozov, Yu. N. Panin, A.I. Fomin and S. M. Chernyavskii, JETP Lett. **57**, 464 (1993).
 - [13] Yu. N. Pokotilovski, M. I. Novopoltsev, P. Geltenbort, and T. Brenner, Instruments and Experimental Techniques, **54**,16 (2011).
 - [14] A. Saunders, M. Makela, Y. Bagdasarova et al., Review of Scientific Instruments **84**, 013304 (2013).
 - [15] Zhehui Wang, C. L. Morris, M. Makela et al., Nuclear Instruments and Methods in Physics Research A **605**, 430 (2009).
 - [16] C. L. Morris, A. Saunders, S. J. Seestrom, et al., submitted to Phys. Rev. B (2013).

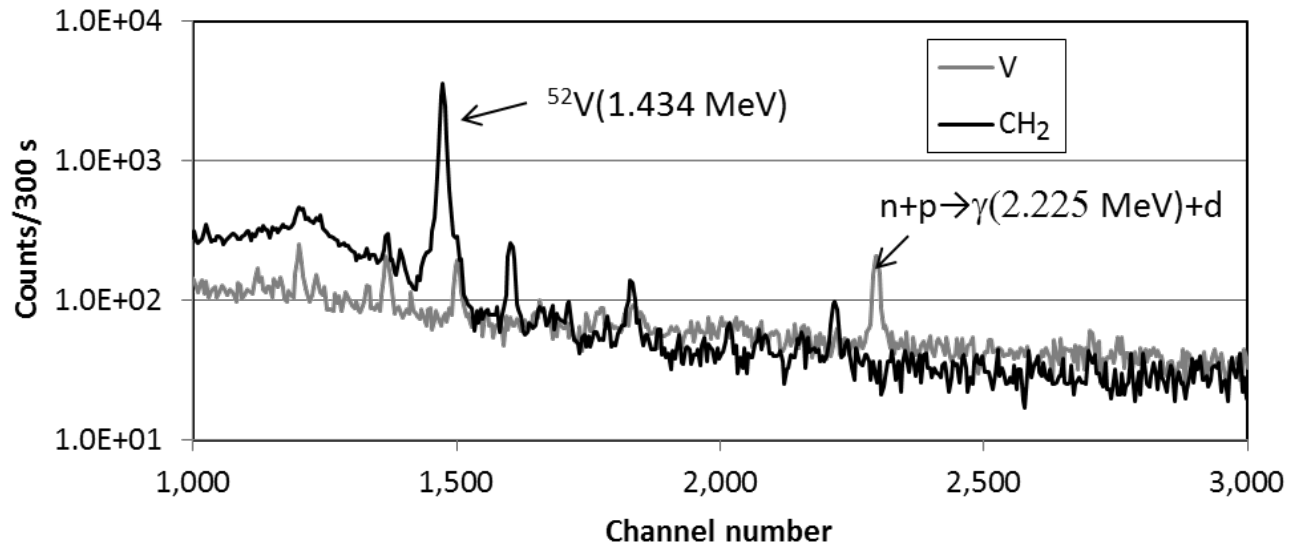


FIG. 1: Pulse height spectra from the ^3He detector for the polyethylene, vanadium and no target. The shoulder on the large pulse height peak and the low pulse height peak are due to wall effects in the detector.

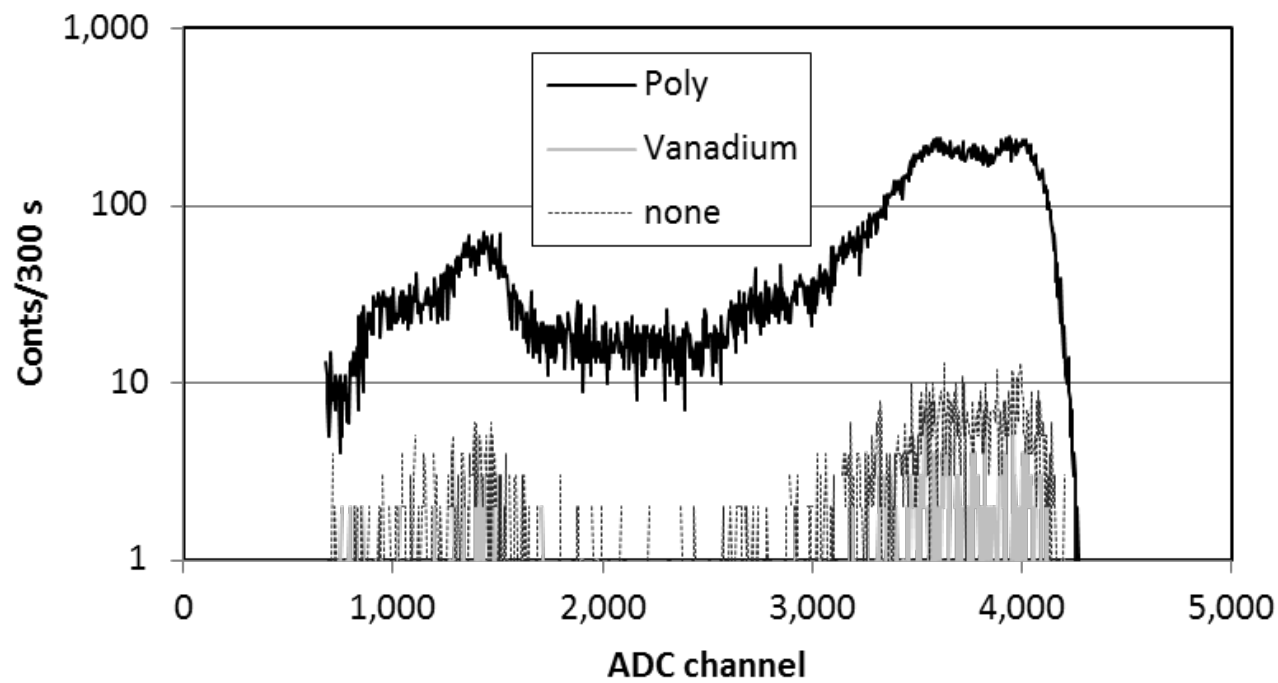


FIG. 2: Gamma ray spectra obtained with UCN. The gamma line from n-p capture with the polyethylene target and the gamma line from the product target ^{52}V are labeled.